RELIABILITY-BASED PREDICTIONS OF A DESIGN AIR GAP FOR FLOATING OFFSHORE STRUCTURES

L. Manuel, M. ASCE

Dept. of Civil Engineering, University of Texas at Austin, Austin, TX 78712
lmanuel@mail.utexas.edu

Steven R. Winterstein, M. ASCE

Dept. of Civil and Environmental Eng., Stanford University, Stanford, CA 94305-4020
steve@ce.stanford.edu

Abstract

The reliability of a floating offshore structure against extreme air gap response levels is studied. A procedure that includes nonlinear diffraction effects under random wave excitation is presented. It permits inclusion of randomness in significant wave height, H_s, in peak spectral period T_p given H_s, and also in the extreme air gap given H_s and T_p. Numerical results are presented by applying these methods to a specific floating structure: a semi-submersible. This semi-submersible is one that is sited in the Northern North Sea. Appropriate joint contours of significant wave height and peak period are developed to establish nominal load levels for use in a load-and-resistance-factor-design (LRFD) procedure.

Introduction

In reliability-based design, the conventional load and resistance factor design (LRFD) procedure involves scaling of a nominal load and resistance, L_{nom} and R_{nom}, by separate load and resistance factors to account for possible under-strength and overloads when checking ultimate/extreme limit states:

$$\phi_R R_{nom} \geq \gamma_L L_{nom} \qquad (1)$$

The nominal load level, L_{nom}, is typically associated with a specified return period (e.g., 100 years). Various definitions of L_{nom} can account for load variability. We define three such loads relating to the extent of the uncertainty preserved in the load/demand used in the checking equation. The key uncertainties in most floating structures exist in the significant wave height (H_s), peak spectral period (T_p), and response (in this study, for instance, our response quantity is the median extreme air gap in a single 3-hour seastate). One definition of L_{nom} might be based, for example, on a representative load associated with the 100-year H_s while neglecting the uncertainty in T_p and response. This definition is not especially interesting for floating structures since, unlike fixed structures that are most sensitive to H_s, floaters are typically sensitive to T_p as well as to potential dynamic amplification resulting from wave sub- and super-harmonics. A second definition might be based on a representative 100-year load including uncertainty in both H_s and T_p, but neglecting uncertainty in the response (given H_s and T_p). We will study two situations of this latter 2D type: in the first, the response is held fixed at its median level; in the second, the response is taken at the 85th percentile level (conditional on H_s and T_p) since this level has been suggested for estimating 100-year loads while recognizing some level of variability in the response. Finally, a definition for L_{nom} could be based on the "true"

100-year nominal load including uncertainty in H_s, T_p, and in response given H_s and T_p. We will refer to this as the "Full-3D" modeling situation in the following.

Obviously, the load factor, γ_L, in Eq. (1) will be appropriately different for each of the nominal load definitions above in order to assure that the design checking equation leads to consistent reliability estimates in each case. Our interest will specifically focus on the two 2D nominal load definitions (50% and 85%) and the "Full-3D" definition. We are also interested in determining whether *ad hoc* adjustments of the simpler-to-estimate and inflated 2D loads can yield consistent reliability levels with those resulting from the use of the "Full-3D" definition. We will study these differences in the context of the design air gap for a semi-submersible and will seek estimates of these nominal loads using a convenient and efficient inverse-FORM formulation (Winterstein et al., 1993).

Response Statistics for Floating Structures – Moments and Extremes

In modeling floating structures, it is common to employ Volterra series to describe the response (output) of these nonlinear systems. The nonlinear system is defined in terms of first- and second-order transfer functions. For floating structures, these transfer functions are obtained from first- and second-order wave diffraction analysis programs such as WAMIT (e.g., WAMIT, 1995).

We start by defining a sea surface elevation, $\eta(t)$, in terms of a sum of sinusoidal components at N distinct frequencies and a one-sided wave spectrum, $S_\eta(\omega)$ and random phases, θ, as follows:

$$\eta(t) = \sum_{k=1}^{N} a_k \cos(\omega_k t + \theta_k) = \mathrm{Re} \sum_{k=1}^{N} A_k \exp(i\omega_k t); \quad A_k = \sqrt{2 S_\eta(\omega_k)\Delta\omega} \exp(i\theta_k) \quad (2)$$

Any response quantity, $x(t)$, may then be described by a second-order Volterra series representation as follows:

$$x(t) = x_1(t) + x_2(t) = x_1(t) + x_{2-}(t) + x_{2+}(t) \quad (3)$$

where $x_1(t)$, $x_{2-}(t)$, and $x_{2+}(t)$ are the first-order, second-order difference-frequency and second-order sum-frequency contributions, respectively, to the response. We can write each of these components in terms of transfer functions. Thus, we have:

$$x_1(t) = \mathrm{Re} \sum_{k=1}^{N} A_k H_k^{(1)} \exp(i\omega_k t)$$

$$x_{2\pm}(t) = \mathrm{Re} \sum_{k=1}^{N} \sum_{l=1}^{N} A_k A_l^{\pm} H_{kl}^{(2\pm)} \exp[i(\omega_k \pm \omega_l)t]; \quad A_l^{+} = A_l; \quad A_l^{-} = A_l^{*}$$

(4)

We will characterize the physical response model and estimate response extremes using the first four statistical moments of the response. One can then express $x(t)$ in terms of mutually independent standard Gaussian processes, $u_j(t)$. Thus, we have:

$$x_1(t) = \sum_{j=1}^{2N} c_j u_j(t); \quad x_2(t) = \sum_{j=1}^{2N} \lambda_j u_j^2(t) \quad (5)$$

The coefficients c_j and λ_j are obtained by solving an eigenvalue problem involving the transfer functions and input power spectral densities (see Kac and Seigert, 1947). To represent the four statistical moments, we will employ the mean (m_x), standard deviation (σ_x), and the dimensionless coefficients of skewness (α_{3x}) and kurtosis (α_{4x}):

$$m_x = E[x(t)]; \quad \sigma_x^2 = E[(x(t) - m_x)^2]$$
$$\alpha_{3x} = E[(x(t) - m_x)^3]/\sigma_x^3; \quad \alpha_{4x} = E[(x(t) - m_x)^4]/\sigma_x^4 \tag{6}$$

In terms of c_j and λ_j in Eq. (5), these first four moments may be found as follows:

$$m_x = \sum_{j=1}^{2N} \lambda_j; \quad \sigma_x^2 = \sum_{j=1}^{2N} (c_j^2 + \lambda_j^2)$$
$$\alpha_{3x} = \frac{1}{\sigma_x^3} \sum_{j=1}^{2N} (6c_j^2 \lambda_j + 8\lambda_j^3); \quad \alpha_{4x} = 3 + \frac{1}{\sigma_x^4} \sum_{j=1}^{2N} (48c_j^2 \lambda_j^2 + 48\lambda_j^4) \tag{7}$$

Once these moments are found, the response process $x(t)$ may be related to a standard Gaussian process $u(t)$ using a Hermite transformation model (Winterstein, 1988):

$$x = m_x + \kappa \sigma_x [u + c_3(u^2 - 1) + c_4(u^3 - 3u)] \tag{8}$$

where c_3, c_4 and κ are coefficients that can be estimated in terms of α_{3x} and α_{4x}. The p-fractile extreme response in a seastate duration T can then be estimated from Eq. (8) taking u as the corresponding Gaussian p-fractile extreme.

Influence of Waves and Structural Motions on Air Gap

We start by defining the net wave elevation, η_{NET}, with respect to a fixed origin. Then, if at a field point of interest, (x,y), $\delta(t)$ denotes the net vertical displacement of the structure, the relative wave elevation $r(t)$ measured with respect to the moving structure may be given by:

$$r(t) = \eta_{NET}(t) - \delta(t); \quad \text{where} \quad \delta(t) = \xi_3(t) + y \cdot \xi_4(t) - x \cdot \xi_5(t) \tag{9}$$

implying that $\delta(t)$ is given in terms of the heave (ξ_3), roll (ξ_4), and pitch (ξ_5), motions. The available air gap $a(t)$ is the difference between the still-water air gap, a_0, and $r(t)$:

$$a(t) = a_0 - r(t) \tag{10}$$

The instantaneous net wave elevation, $\eta_{NET}(t)$, in Eq. (9) is a result of both the incident waves that would occur if the structure were not present, and the diffracted waves that arise because of the presence of the structure that alters the flow field.

$$\eta_{NET}(t) = \eta_{1,NET}(t) + \eta_{2,NET}(t)$$
$$\eta_{1,NET}(t) = \eta_{1,I}(t) + \eta_{1,D}(t); \quad \eta_{2,NET}(t) = \eta_{2,I}(t) + \eta_{2,D}(t) \tag{11}$$

In Eq. (11), we see that in our second-order model, we need to represent the net wave elevation as made up of first- and second-order effects due to both incident and diffracted waves. The first-order incident wave $\eta_{1,I}$ is modeled as a stationary Gaussian process,

and consistent first- and second-order transfer functions for $\eta_{1,D}$, $\eta_{2,I}$, and $\eta_{2,D}$ are calculated from hydrodynamic theory. Specifically, a second-order diffraction code can provide transfer functions directly for $\eta_{2,NET}$. If these are not available and if $\eta_{2,D}$ can be neglected, one may use analytical expressions for $\eta_{2,I}$ available from second-order Stokes theory.

The methodology using Volterra series models and moment-based extreme estimation has been implemented in a post-processing routine (Ude et al., 1996) that uses first- and second-order *force* transfer functions and added mass and damping. The transfer functions combined with stiffness, damping, and inertia properties of the structure provide first- and second-order transfer functions to any response quantity, *x(t)*.

In computing the air gap response, we need to simultaneously include both second-order sum-frequency effects (on the wave surface), and second-order difference-frequency effects (on slow drift motions). The air gap response, as described by Eqs. (9) through (11) above, has been implemented in the formulation based on second-order Volterra series and moment-based extremes models (Manuel and Winterstein, 1998). This routine permits input of either numerical second-order diffraction results or analytical Stokes models of $\eta_{2,I}$ (assuming $\eta_{2,D}$ can be neglected).

Structural Model of Semi-Submersible

The structure chosen for the numerical studies is the Troll semi-submersible. Fig. 1 shows a plan view of the platform that has four columns and plan dimensions, 110m x 110m. The mean water depth is 325 meters. Measurements of air gap were made at seven different field point locations. At these same locations, WAMIT diffraction analyses were performed for waves with different headings and with wave periods ranging from 7.4 to 20.0 seconds. Seven field point locations are indicated on Fig. 1. Comparison of analytical predictions of the air gap with measurements at all these field points is the subject of a separate study (Manuel and Winterstein, in preparation). Results for field point 1 alone (at the mid-point of the platform) are discussed in the numerical studies that follow.

Numerical Studies

Results obtained for the relative wave at field point 1 are summarized in Table 1. Included there are results from three models: the "Full-3D" results include variability in the extreme 3-hour response r_m as well as in H_s and T_p, whereas in the other two cases, r_m is held fixed (at its 85th and 50th percentiles, respectively). Fig. 2 shows a plot of how the 2D-median case design relative wave values may be interpreted. H_s-T_p contours for each return period are tangent to iso-response curves at these design points. For instance, the design relative wave is 24.3 meters for the 100-year return period. As expected, the median (50th percentile) results considerably underestimate the true (3D) results. Use of the 85th percentile, which has been suggested to estimate 100-year loads, offers a clear improvement yet remains slightly unconservative. Of course, a single fractile cannot

match the "true" results across all return periods, as they show inherently more variability (slower decay in Fig. 3). Still higher fractiles will thus be needed to estimate loads with longer return periods (1000-10000 years).

Finally, Table 2 shows the effect of neglecting second-order diffraction contributions as is often done in practice due to the cost of computing these second-order transfer functions. It is clear that this omission can lead to highly unconservative estimates of the relative wave, and thus, the air gap. Note that this conclusion is specific to both this particular (large column) structure, and to this particular (mid-point) location. Lesser second-order effects have been found to be predicted at other field points. Additional comparison of such results with model test behavior is also required, and is a topic of ongoing study.

Conclusions

The reliability of a semi-submersible against extreme air gap reductions has been studied. The Inverse-FORM approach has been employed to estimate the extreme/design air gap levels associate with specified return periods. The importance of the second-order transfer functions due to diffraction is dramatic; exclusion of these can lead to highly unconservative air gap estimates. With regard to defining nominal load levels for a design air gap, the 2D definition, where only H_s and T_p treated as random, is unconservative, even when the 85th percentile of response is employed.

References

Kac, M. and A. J. F. Seigert (1947). "On the Theory of Noise in Radio Receivers with Square Law Detectors," Journal of Applied Physics, Vol. 18, pp. 383-400.

Manuel, L. and S. R. Winterstein (1998). "Estimation of Air Gap Statistics for Floating Structures: Release of TFPOP Version 2.2 – A Computer Program for Performing Stochastic Response Analysis of Floating Structures," Technical Note TN-4, Reliability of Marine Structures Program, Stanford University.

Manuel, L. and S. R. Winterstein (in preparation). "Air Gap Studies on Floating Structures: Modeling Assumptions, Test Data, and Reliability Analysis."

Ude, T. C., S. Kumar, and S. R. Winterstein (1996). "TFPOP 2.1: Stochastic Response Analysis of Floating Structures under Wind, Current, and Second-Order Wave Loads," Technical Report RMS-18, Reliability of Marine Structures Program, Stanford University.

WAMIT, 4.0 (1995). "WAMIT: A Radiation-Diffraction Panel Program for Wave-Body Interaction – Users' Manual," Dept. of Ocean Engineering, M.I.T.

Winterstein, S.R. (1988). "Nonlinear Vibration Models for Extremes and Fatigue," Journal of Engineering Mechanics, ASCE, Vol. 114, No. 10, pp. 1772-1790.

Winterstein, S.R., T.C. Ude, C.A. Cornell, P. Bjerager, and S. Haver (1993). "Environmental Contours for Extreme Response: Inverse FORM with Omission Factors," Proc. ICOSSAR-93, Innsbruck.

Return Period (yrs)	Full-3D			2D & 85%-ile response			2D & 50%-ile response		
	H_s (m)	T_p (sec)	r_m (m)	H_s (m)	T_p (sec)	r_m (m)	H_s (m)	T_p (sec)	r_m (m)
100	11.4	13.2	31.0	13.5	13.6	28.9	13.5	13.6	24.3
1000	12.1	13.4	37.8	14.8	13.8	32.9	14.8	13.8	27.6
10000	12.8	13.5	45.3	15.9	14.0	36.9	16.0	14.0	30.8

Table 1. Design Point (showing extreme relative wave elevation, r_m, a measure of the air gap as given by Eq. 10) for different return periods

Return Period (yrs)	Full-3D		
	H_s (m)	T_p (sec)	r_m (m)
100	11.9	13.4	14.3
1000	12.5	13.4	16.1
10000	13.0	13.5	18.0

Table 2. Design Point where second-order diffraction effects are neglected (compare with Full-3D case in Table 1)
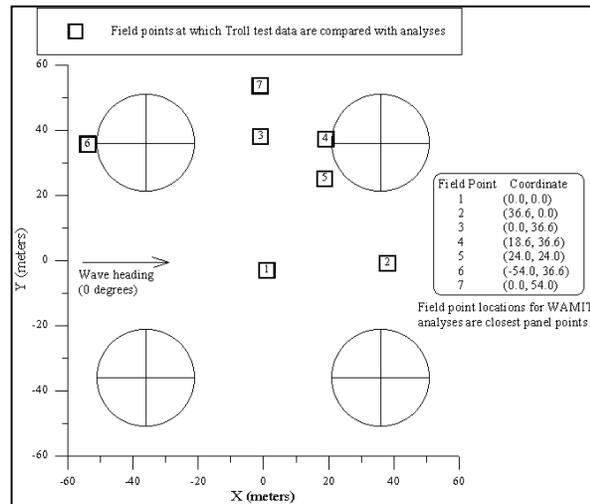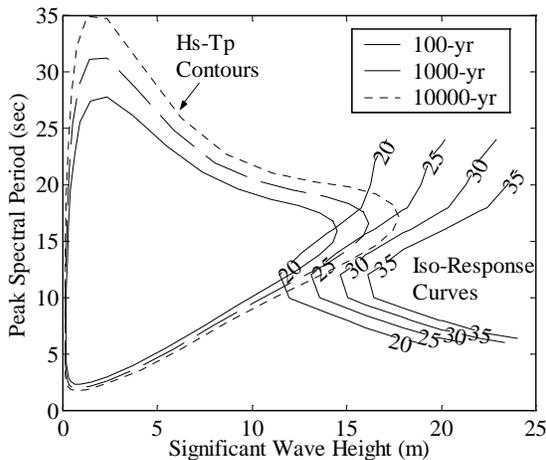

Figure 1. Plan View of the Troll semi-submersible

Figure 2. Iso- esponse curves for different values of median extreme relative wave elevation and H_s-T_p contours for three return periods
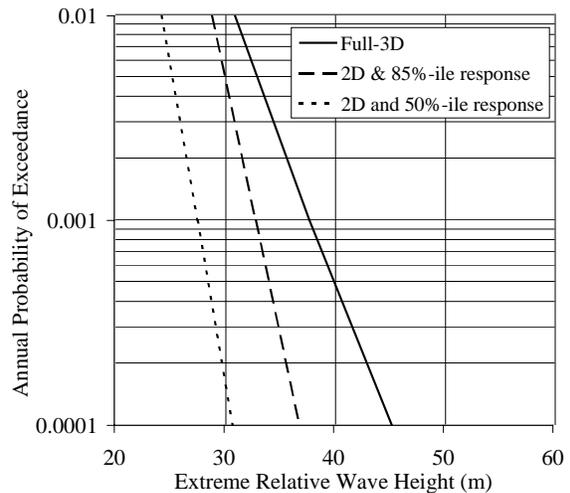

Figure 3. Annual probability of exceedance of different relative wave levels (related to air gap levels)